Upper bounds on collective light-matter coupling strength with plasmonic meta-atoms

Evgeny Ryabkov,[1] Ivan Kharichkin,[1] Sophia Guzik,[1] Alexander Nekhocheninov,[1]
Benjamin Rousseaux,[2,*] and Denis G. Baranov[1,3,†]

[1]*Center for Photonics and 2D Materials, Moscow Institute of Physics and Technology, Dolgoprudny 141700, Russia*
[2]*Laboratoire Interdisciplinaire Carnot de Bourgogne, CNRS UMR 6303, Universite de Bourgogne, BP 47870, 21078 Dijon, France*
[3]*Russian Quantum Center, Moscow 121205, Russia*

(Received 26 December 2022; revised 29 June 2023; accepted 28 July 2023; published 15 August 2023)

Ultrastrong coupling between optical and material excitations is a distinct regime of electromagnetic interaction that enables a variety of physical phenomena. Traditional ways to ultrastrong light-matter coupling involve the use of some sorts of quantum emitters, such as organic dyes, quantum wells, superconducting artificial atoms, or transitions of two-dimensional electron gases. Often, reaching ultrastrong coupling requires special conditions, including high vacuum, strong magnetic fields, and low temperatures. Recent reports indicate that a high degree of light-matter coupling can be attained at ambient conditions with plasmonic meta-atoms—artificial metallic nanostructures that replace quantum emitters. Yet, the fundamental limits on the coupling strength that can be attained with this platform have not been identified. Here, using a Hamiltonian approach we theoretically analyze spectra of polaritonic states and examine the upper limits of the collective plasmon-photon coupling strength in dense assemblies of plasmonic meta-atoms. Starting off with spheres, we identify the universal upper bounds on the normalized collective coupling strength η between ensembles of plasmonic meta-atoms and free-space photons. Next, we examine spheroidal metallic meta-atoms and show that a strongly elongated meta-atom is the optimal geometry for attaining the highest value of the collective coupling strength in the array of meta-atoms. The results could be valuable for the field of polaritonics studies, quantum technology, and modifying material properties.

DOI: 10.1103/PhysRevB.108.075417

I. INTRODUCTION

Strong coupling between two harmonic oscillators—either of classical or quantum nature—is one of the most basic physical models that can be employed to understand the behavior of various mechanical and electromagnetic systems. Polaritons—stationary eigenstates of a coupled system in the strong coupling regime—are hybridized states whose wave function is characterized by the photonic and the matter component simultaneously [1,2]. In the optical domain, polaritonic states are often realized by means of coupling an optical cavity mode with electronic or vibrational transitions in resonant media [2–6]. Thanks to their hybrid composition, optical polaritons manifest unique properties that are typical of simultaneous excitations of light and matter [7]. This offers new ways for modifying the microscopic properties of matter [8–10] and even controlling the rates of chemical reactions [11–16]. The extent to which these microscopic properties can be modified is often determined by the interaction strength between the two components of the coupled system [17–23]. This calls for finding the ways to improve the coupling strength in polaritonic systems.

In the saturation limit—when the entire volume of the cavity is filled with emitters—the key characteristic that determines the resulting interaction constant is the reduced oscillator strength, which is proportional to the transition dipole moment, and the volume density of oscillators in the medium [24–26]. There is a solid theoretical evidence to believe that it is not possible to boost the coupling strength by confining the cavity mode volume—shrinking the cavity mode volume increases the coupling strength with few to individual emitters [27], up to the point where the mode will excite less and less transitions as the volume becomes smaller than the emitters themselves [28–30].

Recent theoretical and experimental efforts have shown that it is possible to boost the coupling strength in polaritonic systems by utilizing so-called meta-atoms—resonant metallic nanoparticles hosting localized plasmonic resonances [31,32]. Despite not having a discrete anharmonic energy ladder like quantum emitters, such meta-atoms participate in the coupling process in a similar way, resulting in the emergence of hybrid polaritonic states with equally spaced (harmonic) energy ladders [33,34]. An additional appeal of meta-atoms is the possibility to design chiral resonant emitters [35,36], which allows engineering and studying the physics of chiral polaritonic states [37,38]. This approach has enabled the exotic regimes of ultrastrong (USC) [39–41] and even deep strong coupling [42] at ambient conditions, which was previously unavailable with more traditional quantum emitter platforms. In these regimes, not only the excited states, but also the ground state of the system experiences a modification upon coupling [43–45].

The experimental progress in realizing polaritonic states with artificial meta-atoms begs a natural question: What is

*benjaminrousseaux@gmail.com
†denis.baranov@phystech.edu

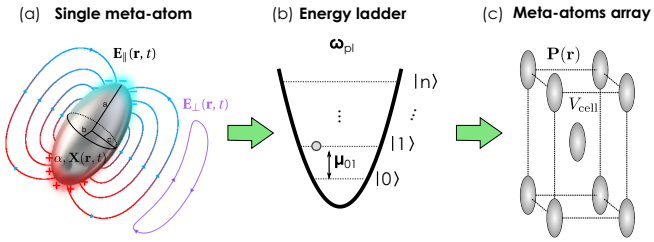

FIG. 1. (a) A single spheroidal metallic nanoparticle as a meta-atom, with semi-axes a, b, and c. The general Power-Zienau-Woolley Hamiltonian [Eq. (2)] is used to describe the meta-atom with polarization $\mathbf{P}(\mathbf{r},t)=\alpha\mathbf{X}(\mathbf{r},t)$. The charge density $\alpha(\mathbf{r})$ is displaced with a vector field $\mathbf{X}(\mathbf{r},t)$. This system couples to the electric field $\mathbf{E}=\mathbf{E}_\parallel+\mathbf{E}_\perp$, where $\mathbf{E}_\parallel=-\nabla\Phi$ is the longitudinal field created by the charge density and $\mathbf{E}_\perp$ is a divergence-less field from either the radiation of the meta-atom or external waves. (b) In the long-wavelength approximation, $\mathbf{P}\approx\boldsymbol{\mu}_{01}(b+b^\dagger)\delta(\mathbf{r}-\mathbf{r}_0)$ with $\boldsymbol{\mu}_{01}$ denoting the transition dipole moment between two consecutive levels of the meta-atom, which is described as a harmonic energy ladder. (c) The same general Hamiltonian (2) is then used in the continuous limit to model the meta-atom array as a density of dipoles per unit volume V_{cell} with inputs ω_{pl} and $\boldsymbol{\mu}_{01}$ from the single meta-atom description.

the upper bound on the coupling strength in polaritonic systems involving meta-atoms? Certain analytical models have been proposed that describe polaritonic states of such system using rigorous coupled-dipoles method [46]. However, that particular model was developed for subwavelength spherical meta-atoms, and as a result cannot be applied to study the limits of plasmon-photon coupling in the case of large spherical or nonspherical particles.

In this paper, using a Hamiltonian approach we theoretically analyze spectra of polaritonic states and examine the upper limits of the collective plasmon-photon coupling strength in dense assemblies of plasmonic meta-atoms. Starting with the case of analytically solvable spherical meta-atoms, we identify the universal upper bounds on the normalized collective coupling strength (denoted η in the following) between ensembles of plasmonic meta-atoms and free-space photons. Then, with the aid of numerical simulations, we examine the case of spheroidal meta-atoms. Our results suggest that strongly elongated meta-atoms could be the optimal geometry for attaining the highest value of the collective coupling strength with the optical field.

II. SYSTEM UNDER STUDY

The system we analyze in this study is represented by an ensemble of (generally) spheroidal metallic meta-atoms with semi-axes a, b, and c, and permittivity $\varepsilon_m(\omega)$ distributed in a host medium (air), Fig. 1. The meta-atoms are assumed to be distributed in space periodically, with volume filling factor f defined as a ratio of the volume occupied by the metallic fraction to the total volume of the system, $f=V_{\text{metal}}/V$.

The permittivity of metallic meta-atoms is described by the Drude model,

$$\varepsilon_m(\omega)=\varepsilon_\infty-\frac{\omega_P^2}{\omega(\omega+i\gamma_D)}, \tag{1}$$

where ω_P is the plasma frequency of the metal, ε_∞ is the high-frequency permittivity accounting for the interband transitions, and γ_D is the electron collision rate. For the sake of simplicity, we will ignore dissipation in this study and assume $\gamma_D=0$. Each meta-atom supports a localized plasmon resonance associated with oscillations of the electron density of the particle. The resulting ensemble of plasmonic meta-atoms interacts with a photon of energy $\hbar\omega_{\mathbf{k}}$ propagating across the surrounding medium, which is assumed to be air ($\varepsilon=1$).

In order to describe the polaritonic spectrum of the system, we will develop in the following a Hamiltonian model involving the matter polarization. For simplicity, we describe the interaction of the localized oscillators' dipolar transitions with the transverse photonic field, which can be generalized to multipolar transitions.

III. HAMILTONIAN MODEL OF THE SYSTEM

A. General Power-Zienau-Woolley Hamiltonian

To describe the interaction between the cubic lattice of meta-atoms and the transverse photonic field, we use a Hamiltonian formulation in the Power-Zienau-Woolley representation of the Coulomb gauge. The authors of Ref. [46] previously developed a model of the plasmon-photon interaction in the Coulomb gauge that accurately takes into account the near-field Coulomb interaction between meta-atoms. The resulting model, in particular, captures the anisotropy of the polaritonic modes induced by the internal anisotropy of the cubic lattice of the meta-atoms. However, the limits to the plasmon-photon coupling have not been analyzed.

Here, we are aiming at a simplified model that would allow us to easily characterize the strength of plasmon-photon coupling in densely packed cubic arrays. To that end, we start from the Power-Zienau-Woolley (or multipolar) representation, wherein the mutual multipolar interactions between the meta-atoms are accounted for by the quadratic self-polarization term. Considering an ensemble of meta-atoms, each of volume V_j and single resonance frequency ω_j, we show in Appendix A that the Hamiltonian

$$\begin{aligned}H=&\underbrace{\sum_j\int_{V_j}d^3r\left(\frac{\boldsymbol{\Pi}_j^2}{2\rho}+\frac{1}{2}\rho\omega_j^2\mathbf{X}_j^2\right)}_{\text{meta-atoms}}\\&+\underbrace{\int_{\mathbb{R}^3}d^3r\left(\frac{\boldsymbol{\Pi}_A^2}{2\epsilon_0}+\frac{(\nabla\times\mathbf{A})^2}{2\mu_0}\right)}_{\text{radiation}}\\&+\underbrace{\sum_j\int_{V_j}d^3r\frac{\mathbf{P}_j^2}{2\epsilon_0}}_{\mathbf{P}^2\text{-term}}+\underbrace{\sum_j\int_{V_j}d^3r\frac{\mathbf{P}_j\cdot\boldsymbol{\Pi}_A}{\epsilon_0}}_{\text{interaction}}\end{aligned} \tag{2}$$

generates the source-free Maxwell's equations $\nabla\cdot\mathbf{D}=0$, $\nabla\cdot\mathbf{B}=0$, $\nabla\times\mathbf{E}=-\frac{\partial}{\partial t}\mathbf{B}$, $\nabla\times\mathbf{H}=\frac{\partial}{\partial t}\mathbf{D}$, as well as the equation of motion of the macroscopic polarization $\mathbf{P}=\sum_j\mathbf{P}_j$,

$$\left(\frac{\partial^2}{\partial t^2}+\omega_j^2\right)\mathbf{P}_j(\mathbf{r},t)=\beta_j(\mathbf{r})\mathbf{E}(\mathbf{r},t), \tag{3}$$

where $\beta_j(\mathbf{r}) = \alpha_j(\mathbf{r})/\rho$, ρ being the carrier volumic mass in the medium of the resonators, and $\alpha_j(\mathbf{r})$ being the displaced carrier density in resonator j, Fig. 1(a). The displacement of the carriers is contained in the vector field $\mathbf{X}_j(\mathbf{r}, t)$, whose canonical momentum is $\mathbf{\Pi}_j = \rho \frac{\partial}{\partial t}\mathbf{X}_j$. The radiation field with vector potential $\mathbf{A}$ and canonical momentum $\mathbf{\Pi}_A = -\mathbf{D}$ is purely transverse in the Coulomb gauge. We emphasize that in the picture given by Hamiltonian (2), Ohmic dissipation is disregarded. A more rigorous treatment with additional degrees of freedom in the Hamiltonian would provide a description of the Ohmic losses, but is beyond the scope of this paper. The general form of Hamiltonian (2) is used to treat both the cases of (1) a single meta-atom coupling to the radiation field, and (2) a periodic array of densely-packed meta-atoms, with input parameters from the single meta-atom description.

We emphasize that in determining upper bounds for the collective coupling strength of an array of meta-atoms, we restrict our study to dipolar plasmonic modes of the individual meta-atoms. In the limit of close packing, however, higher-order multipoles and their mutual interaction must generally be accounted. A first, natural step would consist in including quadrupoles [47]. However, the inclusion of multipoles introduces many coupling strengths to be investigated, which is beyond the scope of this paper.

B. Meta-atom transition dipole moments

One important ingredient of the Hamiltonian model of the optical field–meta-atom interaction is the transition dipole moment of an individual meta-atom. To that end, we consider a single meta-atom in free space and employ the classical theory of light scattering in order to evaluate its transition dipole moment matrix element.

The quasinormal mode of a single plasmonic meta-atom can essentially be described as a harmonic oscillator with an equidistant energy ladder, see Fig. 1(b). In the spirit of cavity QED dealing with subwavelength two-level quantum emitters, such as electronic and vibrational transitions of atoms and molecules, we will characterize the transitions between each pair of eigenstates $n \to n+1$ by the transition dipole moment (TDM) matrix element $\boldsymbol{\mu}_{\mathrm{mn}}$. We restrict our analysis to the low-energy domain of the oscillator represented by the $0 \to 1$ transition of the meta-atoms. Particularly, the radiative transition between the ground $|0\rangle$ and the first excited $|1\rangle$ Fock states of the plasmonic meta-atom is quantified by

$$\boldsymbol{\mu}_{01} = \langle 0|q\mathbf{r}|1\rangle, \tag{4}$$

where $\mathbf{r}$ is the position operator corresponding to the center-of-mass motion of the electron cloud for the dipolar plasmon, with total charge q.

Although the system, generally, consists of spheroidal meta-atoms, we begin our analysis with the special case of spherical meta-atoms, whose properties can be described by closed-form analytical expressions. To quantify these dipole transitions, we first find complex eigenfrequencies of the TM_1 quasinormal modes of the metallic sphere. These eigenfrequencies can be found numerically as roots of the characteristic equation [48]

$$n\psi_l(nx)\xi_l'(x) - \xi_l(x)\psi_l'(nx) = 0, \tag{5}$$

where $x = k_0 r$, $\psi_l(x) = x j_l(x)$, and $\xi_l(x) = x h_l^{(1)}(x)$ are Ricatti-Bessel functions, and $j_l(x)$ and $h_l^{(1)}(x)$ are spherical Bessel and Hankel functions of the first kind, respectively.

Once the complex-valued eigenfrequencies $\widetilde{\omega} \equiv \omega_{pl} - i\gamma_{pl}/2$ of the electric dipole quasinormal modes of the meta-atoms are determined, one can calculate their transition dipole moments $|\boldsymbol{\mu}_{01}|$ by applying the spontaneous decay rate formula [49]

$$\gamma_{pl} = \frac{\omega_{pl}^3}{3\pi\hbar\varepsilon_0 c^3}|\boldsymbol{\mu}_{01}|^2. \tag{6}$$

Although this expression is traditionally used to describe radiative decay rate of two-level systems, it can be equally applied to describe the transition rates between the equidistant levels of a harmonic multi-level emitter. Using Fermi's golden rule, we show in Appendix B that restricted to a single meta-atom, the Hamiltonian (2) yields Eq. (6).

C. Densely packed meta-atom array Hamiltonian

Next we consider a three-dimensional array of identical meta-atoms whose individual transition dipole moments $\boldsymbol{\mu}_{01}$ are assumed to be aligned, Fig. 1(c). Assuming a densely packed array, we are going to derive the Hamiltonian of the system in the continuous limit, but we first need to express the polarization operator. The latter corresponds to the density of dipoles per unit volume, and since the system is periodic, it is

$$\mathbf{P}(\mathbf{r}) = \sum_{j=1}^{N} \frac{\boldsymbol{\mu}_{01}}{V_{\mathrm{cell}}}(a_j + a_j^\dagger), \tag{7}$$

where V_{cell} is the unit-cell volume of the lattice, $N = fV_{\mathrm{cell}}/(\frac{4}{3}\pi abc)$ is the number of meta-atom in the unit cell, and $a_j, a_j^\dagger$ are the (bosonic) annihilation and creation operators satisfying the commutation relations $[a_j, a_k^\dagger] = \delta_{jk}$ and corresponding to the dipolar excitation of an individual meta-atom. All the dipoles within the unit cell can be viewed as a single effective dipole $\boldsymbol{\mu}_N = \sqrt{N}\boldsymbol{\mu}_{01}$, by defining a collective bosonic operator $b = \frac{1}{\sqrt{N}}\sum_{j=1}^{N} b_j$, yielding

$$\mathbf{P}(\mathbf{r}) = \frac{\boldsymbol{\mu}_N}{V_{\mathrm{cell}}}(b + b^\dagger). \tag{8}$$

We now perform the continuous limit, i.e., we describe the array as a density of dipoles with a polarization expanded in the plane-wave basis [50]

$$\mathbf{P}(\mathbf{r}) = \sum_{\mathbf{Q}} \frac{\boldsymbol{\mu}_N}{V_{\mathrm{cell}}} \mathrm{e}^{-i\mathbf{Q}\cdot\mathbf{r}}(b_{\mathbf{Q}} + b_{-\mathbf{Q}}^\dagger) \tag{9}$$

In the above formula, $b_{\mathbf{Q}}, b_{\mathbf{Q}}^\dagger$ are bosonic annihilation and creation operators for a matter excitation propagating with wave vector $\mathbf{Q}$ in the array. The matter Hamiltonian H_{mat}, containing the bare meta-atom and $\mathbf{P}^2$ parts of Eq. (2) is then, for a given $\mathbf{Q}$,

$$H_{\mathrm{mat}} = \hbar\omega_{pl} b_{\mathbf{Q}}^\dagger b_{\mathbf{Q}} + \frac{\boldsymbol{\mu}_N^2}{2\epsilon_0 V_{\mathrm{cell}}}(b_{\mathbf{Q}} + b_{-\mathbf{Q}}^\dagger)(b_{-\mathbf{Q}} + b_{\mathbf{Q}}^\dagger), \tag{10}$$

where $\omega_{pl} \equiv \omega_j$ is the resonance frequency of a single meta-atom when ignoring its interaction with light.

TABLE I. The list of different energetic quantities involved in the problem of collective meta-atom-photon coupling.

Quantity	Physical meaning
$\omega_{\mathbf{k}}$	Photon frequency
ω_{pl}	Meta-atom resonant frequency
γ_{pl}	Meta-atom decay rate
Ω_{pl}	Renormalized meta-atom frequency
$g_{\mathbf{k}}$	Collective coupling strength
η	Normalized collective coupling strength
$\widetilde{g}_{\mathbf{k}}$	Rescaled coupling strength
$\Omega_{\pm}$	Polaritonic transition frequencies
Ω	Mode splitting
$\overline{\omega}$	Upper edge of polariton gap
$\underline{\omega}$	Lower edge of polariton gap
Δ_{pol}	Polariton gap

Diagonalization of the matter Hamiltonian, $H_{\text{mat}} \to \hbar\Omega_{pl} B^{\dagger}_{\mathbf{Q}} B_{\mathbf{Q}}$, yields the renormalized eigenfrequency of the meta-atom array,

$$\Omega_{pl} = \sqrt{\omega_{pl}^2 + 2\frac{\boldsymbol{\mu}_N^2}{\hbar\epsilon_0 V_{\text{cell}}}\omega_{pl}}. \tag{11}$$

For reference, Table I lists the physical meaning of different energetic quantities involved in the problem.

D. Collective light-matter coupling

We next focus on the light-matter interaction term, assuming the array is homogeneous in the dipole orientation, along the z axis. In the original basis, involving the operators $b_{\mathbf{Q}}$, $b^{\dagger}_{\mathbf{Q}}$, the interaction term corresponding to the last term of Eq. (2) takes the form

$$H_{\text{light-mat}} = -i\hbar g_{\mathbf{k}}(a_{\mathbf{k}} - a^{\dagger}_{-\mathbf{k}})(b_{-\mathbf{k}} + b^{\dagger}_{\mathbf{k}}), \tag{12}$$

where $a_{\mathbf{k}}$ is the annihilation operator for a transverse magnetic photon with wave vector $\mathbf{k}$ and frequency $\omega_k = c|\mathbf{k}|$, and the array excitation wave vector $\mathbf{Q}$ must now match the photon wave vector $\mathbf{k}$. The *collective* coupling constant is given by

$$\hbar g_{\mathbf{k}} = \mathcal{E}_{\text{vac}}(\mathbf{k})\boldsymbol{\mu}_N \cdot \boldsymbol{\epsilon}_{\mathbf{k}} \tag{13}$$

where

$$\mathcal{E}_{\text{vac}}(\mathbf{k}) = \sqrt{\hbar\omega_{\mathbf{k}}/(2\varepsilon_0 V_{\text{cell}})} \tag{14}$$

is the vacuum electric field of the photonic mode confined to the quantization box of volume V_{cell} and $\boldsymbol{\epsilon}_{\mathbf{k}}$ is the unit transverse magnetic polarization vector. Plugging the vacuum field into Eq. (13) allows us to express the collective coupling constant via the photon frequency, transition dipole moment, and the meta-atoms spatial density,

$$g_{\mathbf{k}} = \sqrt{\frac{f}{V_0}\frac{\omega_{\mathbf{k}}}{2\hbar\varepsilon_0}}\boldsymbol{\mu}_{01} \cdot \boldsymbol{\epsilon}_{\mathbf{k}} \tag{15}$$

where V_0 is the geometric volume of a single meta-atom. In turn, Eq. (15) allows us to express the renormalized meta-atom eigenfrequency in a more compact form

$$\Omega_{pl} = \sqrt{\omega_{pl}^2 + 4g_{\text{res}}^2}, \tag{16}$$

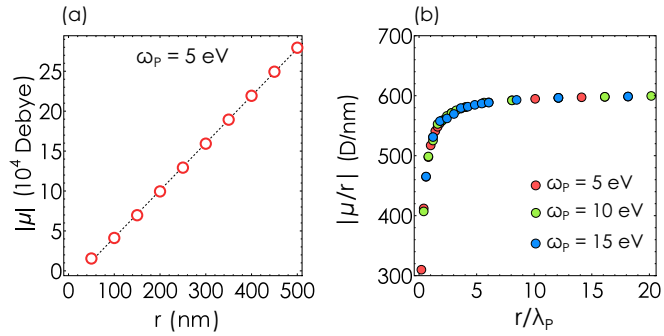

FIG. 2. (a) Magnitude of the transition dipole moment $|\boldsymbol{\mu}_{01}|$ of spherical plasmonic meta-atoms as a function of the meta-atom radius r described by the Drude permittivity, Eq. (1), for $\omega_P = 5$ eV and $\varepsilon_\infty = 1$. The values were calculated by locating poles of the characteristic equation, Eq. (5), and applying Eq. (6). (b) Normalized transition dipole moments $|\boldsymbol{\mu}_{01}|/r$ as a function of the dimensionless radius r/λ_P for three values of the plasma frequency.

where g_{res} is the resonant coupling constant at zero detuning, $\omega_{\mathbf{k}} = \omega_{pl}$, and when the photon polarization $\varepsilon_{\mathbf{k}}$ is aligned with the dipole moment $\boldsymbol{\mu}_{01}$ of the meta-atoms.

In the new basis involving the diagonalized matter part, the Hamiltonian is, for a given wave vector $\mathbf{k}$,

$$H = \hbar\omega_k a^{\dagger}_{\mathbf{k}} a_{\mathbf{k}} + \hbar\Omega_{pl} B^{\dagger}_{\mathbf{k}} B_{\mathbf{k}} - i\hbar\widetilde{g}_{\mathbf{k}}(a_{\mathbf{k}} - a^{\dagger}_{-\mathbf{k}})(B_{-\mathbf{k}} + B^{\dagger}_{\mathbf{k}}), \tag{17}$$

where $\widetilde{g}_{\mathbf{k}} = g_{\mathbf{k}}\sqrt{\omega_{pl}/\Omega_{pl}}$ is the rescaled coupling strength resulting from the first diagonalization step. The full diagonalization of the light-matter Hamiltonian is detailed in the Appendixes C and D. The eigenenergies of the total Hamiltonian take the form

$$E = E_{\text{vac}} + \hbar n\Omega_+ + \hbar m\Omega_-, \quad n, m = 0, 1, 2, \ldots \tag{18}$$

where $\Omega_{\pm}$ denote the resonant *transition* frequencies of the polaritonic system given by the eigenvalues of the Hopfield matrix associated to the Hamiltonian (17),

$$\Omega_{\pm} = \frac{\sqrt{\omega_{\mathbf{k}}^2 + \Omega_{pl}^2 \pm \sqrt{\left(\omega_{\mathbf{k}}^2 - \Omega_{pl}^2\right)^2 + 16\widetilde{g}_{\mathbf{k}}^2\omega_k\Omega_{pl}}}}{\sqrt{2}}, \tag{19}$$

and $E_{\text{vac}} = \hbar(\Omega_+ + \Omega_-)/2$ is the zero-point energy. The mode splitting Ω calculated as the energy difference between the two polaritonic modes at zero detuning takes the form

$$\Omega = \Omega_+ - \Omega_- = 2g_{\text{res}}. \tag{20}$$

IV. RESULTS

A. Transition dipole moments of spherical meta-atoms

Figure 2(a) shows the resulting transition dipole moments of a spherical metallic meta-atom as a function of the meta-atom radius evaluated for the value of plasma frequency $\omega_P = 5$ eV. The plot reveals a nearly linear dependence of the transition dipole moment on the meta-atom radius. The result for a series of other plasma frequencies (10 and 15 eV) shows an analogous behavior (see Fig. S1 within the Supplemental Material, SM [51]). This linear dependence is confirmed by

the fit of the dipole moment in the double-logarithmic scale, Fig. S1. We have checked that the linear dependence remains valid at large meta-atom radius, up to 5 microns, see Fig. S2 within the SM [51]. For completeness, we also show in Fig. S3 within the SM [51] the corresponding resonant frequencies $\Re\mathrm{e}[\widetilde{\omega}] = \omega_{\mathfrak{pl}}$ of the electric dipole quasinormal modes of meta-atoms.

One can notice that for any fixed value of filling factor f there are only two independent dimensional parameters with units of length entirely determining the problem with an individual meta-atom: the meta-atom's radius r, and the plasma frequency ω_P, which can be translated to the corresponding plasma wavelength $\lambda_P = 2\pi c/\omega_P$. This suggests that the normalized radius r/λ_P may play the role of a dimensionless parameter, which could determine all dimensionless characteristics of the meta-atom. To verify this hypothesis, we plot in Fig. 2(b) the normalized transition dipole moment μ_{01}/r as a function of the dimensionless radius r/λ_P, and merge the data series for all three plasma frequencies we have studied. The result clearly shows that the normalized transition dipole moments follow the same dependence with variation of r/λ_P, and approach a universal constant for large r/λ_P irrespective of the plasma frequency of the underlying material.

Overall, the data presented above indicates that the transition dipole moment of large plasmonic meta-atoms scales linearly with radius. To corroborate this asymptotic behavior, we propose a simple analytical estimation of the transition dipole moment. In the limit of large radii of the metallic sphere its fundamental TM_1 (electric dipole) resonance gradually shifts towards long wavelengths, $\lambda_{pl} \to \infty$. In this limit Drude metal described by Eq. (1) turns into a perfect electric conductor with $\Re\mathrm{e}[\varepsilon] < 0$, $|\varepsilon| \gg 1$, and the metallic nanoresonator turns into a dipole antenna [52]. Correspondingly, all dimensional characteristics of the antenna's resonance—such as the resonant wavelength and inverse linewidth—start to scale linearly with the radius [53,54]: $\lambda_{pl} = Ar$, $2\pi c/\gamma = Br$, where A and B are dimensionless parameters.

Since they are dimensionless and at this point there is only one quantity with the units of length left—plasma wavelength λ_P—the constants A and B cannot depend on the plasma frequency of the Drude metal. In turn, this scaling leads to a constant quality factor of the resonance for large radii,

$$Q = \frac{\omega_{pl}}{\gamma_{pl}} \to \frac{B}{A} = \text{const}, \tag{21}$$

which is independent of the plasma frequency. Figure S5 (within the SM [51]) showing the radius dependence of the Q factors of spherical meta-atoms, confirms this statement.

Plugging these asymptotic dependencies into Eq. (6) and resolving it with respect to μ_{01}, we obtain the linear scaling of transition dipole moment of the metallic sphere with radius,

$$\mu_{01} = \sqrt{\frac{A^3}{B}\frac{3\hbar\varepsilon_0 c}{4\pi}}\, r, \tag{22}$$

which agrees with the behavior shown in Fig. 2. Alternatively, we can express the transition dipole moment from Eq. (6) in terms of the meta-atom Q factor. The result takes the form

$$\mu_{01} = \sqrt{AB\frac{3\hbar\varepsilon_0 c}{4\pi}}\,\frac{r}{Q}. \tag{23}$$

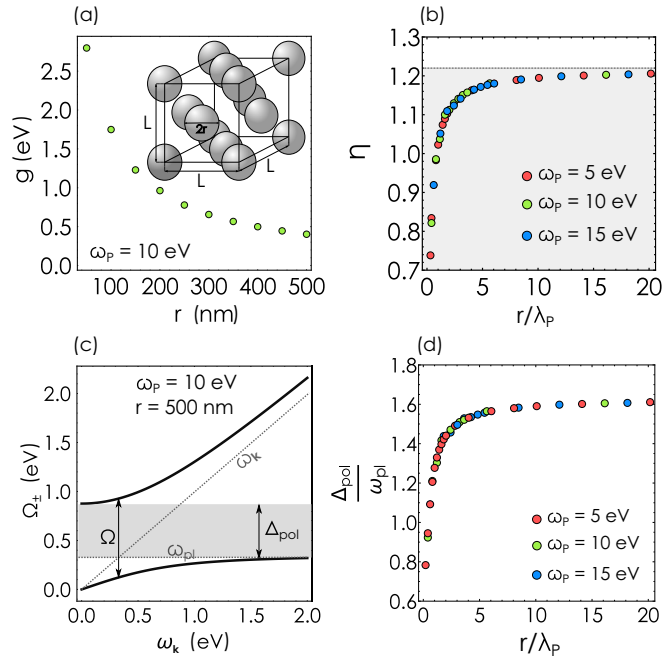

FIG. 3. (a) Collective light-matter coupling strength $g_{\mathbf{k}}$ in the array of densely packed spherical plasmonic meta-atoms as a function of the meta-atom radius r for the fixed filling factor of $f = 0.74$. Inset: Geometry of the periodic system incorporating spherical meta-atoms: a periodic ensemble of metallic spherical meta-atoms of radius r forming an FCC lattice with the lattice constant L. (b) Normalized collective coupling strength $\eta = g_{\mathbf{k}}/\omega_{pl}$ for spherical meta-atoms as a function of the dimensionless radius r/λ_P. The values for a series of plasma frequencies are shown. (c) An exemplary spectrum of polaritonic eigenenergies, Eq. (19), calculated for an array of spherical meta-atoms for $\omega_P = 10$ eV and the meta-atom radius $r = 500$ nm. Shaded area denotes the polariton gap with no allowed real-valued energies. (d) Normalized value of the polariton gap $\Delta_{\mathrm{pol}}/\omega_{pl}$ as a function of the dimensionless radius r/λ_P for three values of the plasma frequency.

This expression will be useful in the following analysis of the collective coupling strength in the arrays of meta-atoms. Additionally, Fig. S6 (within the SM [51]) shows the diameter-to-resonant wavelength ratio $2r/\lambda_{pl}$ for spherical meta-atoms, confirming linear scaling of the resonant wavelength with radius.

B. Polaritonic spectra with spherical meta-atoms

Having calculated transition dipole moments of individual meta-atoms, we now turn to the analysis of the collective polaritonic states in densely packed meta-atom ensembles. For the following we assume that spherical meta-atoms occupy the sites of a three-dimensional face centered cubic (FCC) lattice with a lattice constant L, Fig 3(a). For the FCC lattice of spheres of radius r and center-to-center distance L, the filling factor is given by

$$f = 4\frac{4\pi r^3}{3L^3}. \tag{24}$$

The closest configuration of spheres in such lattice can be reached for $L = 2r\sqrt{2}$, when Eq. (24) recovers the famous

filling factor of an array of closely packed spheres, $f_0 = \pi/(3\sqrt{2}) \approx 0.74$. The resulting system closely resembles the structure realized in Ref. [42].

Figure 3(a) shows the resulting unscaled collective plasmon-photon coupling strength $g_{\mathbf{k}}$ as a function of the meta-atom radius evaluated for $\omega_P = 10$ eV at the zero-detuning condition ($\omega_{\mathbf{k}} = \omega_{pl}$). The resulting coupling strength monotonically decreases with the radius of single meta-atom. A more interesting behavior is found when we plot the *normalized* coupling strength $\eta = g_{\mathbf{k}}/\omega_{pl}$ versus the normalized radius r/λ_P for all three plasma frequencies, Fig. 3(b).

Similarly to Fig. 2(b), normalized coupling strengths obtained for different plasma frequencies follow the same common dependence. This plot clearly shows that even relatively small meta-atoms easily reach the regime of ultrastrong light-matter coupling with $\eta > 0.5$. This is the regime of interaction in which the standard quantum optical approximations, such as the rotating wave approximation, fail. Thus so-called fast-rotating terms, as well as the quadratic P^2 term (or, alternatively, the A^2 term of the Hamiltonian before the PZW transformation) must be taken into account in order to correctly describe the system's behavior [43,55–57]. More remarkably, Fig. 3(b) reveals even more exotic domain of deep strong coupling, commonly defined as the regime of interaction with $\eta > 1$ [44,58,59]. The data suggests that transition to this regime occurs close to $r = \lambda_P$; whether this is the exact threshold or not, should be the subject of a more accurate analytical treatment.

Another remarkable feature of the data in Fig. 3(b) is that the normalized coupling strength η asymptotically approaches a constant (the same for all plasma frequencies) in the limit of large radius,

$$\eta \leqslant 1.2. \tag{25}$$

Since the data points obtained for different plasma frequencies follow the same dependence, this suggests that this upper bound is universal for all plasma frequencies and depends only on the filling factor and the meta-atom shape, which we are going to address below.

This asymptotic behavior can be understood on account of the linear scaling of transition dipole moments in the limit of large radii that is reported in Fig. 2. Indeed, taking into account the asymptotic behaviors of the resonant meta-atom energy ω_0, transition dipole moment μ, and combining it with the physical meta-atom volume V_0, we obtain that the normalized coupling strength approaches a constant,

$$\frac{g_{\mathbf{k}}}{\omega_{pl}} \to \frac{3A\hbar}{8\pi}\sqrt{\frac{B}{\pi}}\frac{\sqrt{f}}{Q} = \text{const}. \tag{26}$$

This simple argument does not, however, allow us to estimate the exact value of the upper limit for the normalized collective coupling strength, which would require a more microscopic treatment of the problem.

Using the obtained coupling strengths we present a typical spectrum of polaritonic eigenenergies $\Omega_\pm$ of an fcc array of meta-atoms with $\omega_P = 10$ eV and $r = 500$ nm, Fig. 3(c). The dispersion features a familiar anticrossing picture with a mode splitting of $\Omega = 2g \approx 0.8$ eV. Figure 3(c) also exhibits

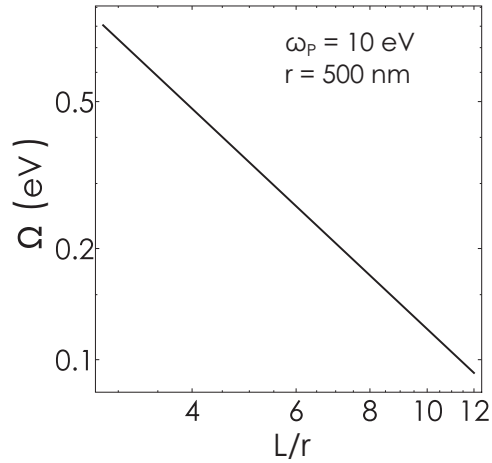

FIG. 4. Mode splitting Ω in an array of $r = 500$ nm and $\omega_P = 10$ eV spherical meta-atoms as a function of the center-to-center distance L/r. Even for diluted structures with $L/r > 10$ the mode splitting remains well above the characteristic nonradiative plasmon decay rate of 50 meV.

a polaritonic gap—a region of energies with no polaritonic states within it [60]. Polariton gap can be interpreted as the Reststrahlen band of the material: the domain of energies wherein the real part of the permittivity becomes negative, thus forbidding propagation of plane waves [25,55].

The lower edge of this gap $\underline{\omega}$ is found to be $\underline{\omega} = \sqrt{\Omega_{pl}^2 - 4g_{\text{res}}^2\Omega_{pl}/\omega_{pl}}$. The upper edge $\overline{\omega}$ is obtained by calculating the upper polariton energy in the limit $k = 0$ and is found to be exactly the rescaled matter frequency $\overline{\omega} = \Omega_{pl}$. The width of the polariton gap therefore is

$$\Delta_{\text{pol}} = \overline{\omega} - \underline{\omega}. \tag{27}$$

Figure 3(d) presents the normalized width of the polariton gap $\Delta_{\text{pol}}/\omega_{pl}$ as a function of the normalized radius r/λ_P for the three studied plasma frequencies. Like in other instances, all data series follow a common dependence, once again highlighting the key role of the dimensionless radius of the meta-atom in this coupling problem.

Although our Hamiltonian model does account for the interparticle Coulomb interactions, it may become less suitable for closely packed lattices with touching particles, when the higher-order multipole interactions beyond the dipole-dipole one may become dominating. For this reason we apply the developed formalism for meta-atom lattices with smaller filling factors. Figure S7 (within the SM [51]) shows more examples of polaritonic energy spectra calculated for the same meta-atoms using smaller values of filling factor f. Expectedly, the mode splitting get smaller with decreasing filling factor as less and less meta-atoms occupy the same volume. Figure 4 shows the mode splitting Ω as a function of the center-to-center interparticle distance a/r. Even for the center-to-center interparticle distance $a = 10r$ corresponding to the moderate value of the filling factor $f = 0.0167$ the mode splitting in the ensemble of $r = 500$ nm meta-atoms reaches a sizable fraction of the resonant energy, $\Omega \approx 0.2\omega_{pl}$, and remains well above 50 meV, which is the characteristic

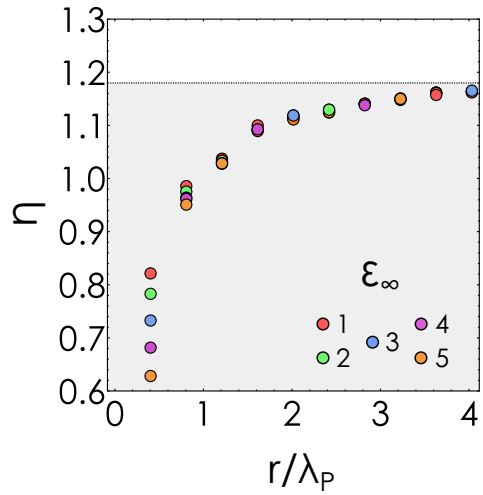

FIG. 5. The effect of the screening dielectric constant ε_∞ on the collective coupling strength of spherical meta-atoms for closely packed lattice with $f = 0.74$.

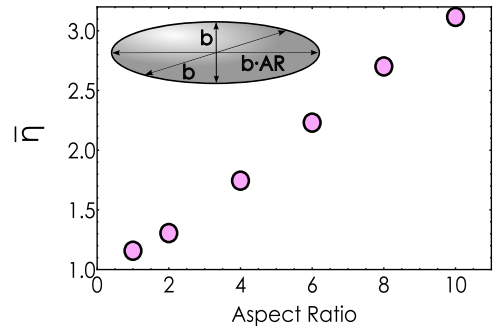

FIG. 6. The attainable maximum $\bar{\eta}$ of normalized collective coupling strength between the fundamental electric dipole transition of spheroid meta-atoms and free-space photonic field for closely packed arrays of metallic spheroids ($f = 0.74$) as a function of the spheroid AR. The data is obtained for a fixed plasma frequency $\omega_P = 10$ eV. Inset: Geometry of the modified meta-atom, represented by a prolate spheroid metallic meta-atoms with the long axis a and shorter axis b.

nonradiative decay rate for plasmonic metals such as Ag and Au.

Similarly, the geometry of the unit cell will affect the polaritonic spectrum; however, it can be easily accounted for by plugging an appropriate filling factor f in the coupling constant g_k.

Before moving on to nonspherical meta-atoms, we briefly investigate the effect of the screening constant ε_∞ on the collective coupling strength. Figure 5 presents the resulting normalized collective coupling η as a function of the normalized meta-atom radius r/λ_P for a few values of ε_∞ typical for plasmonic metals. For small meta-atoms, $r < \lambda_P$, the collective coupling is affected significantly by the dielectric screening. In the limit of large meta-atoms, however, the normalized coupling constant asymptotically approach the same value of $\approx$1.2 irrespective of the screening constant ε_∞. It can be understood by the virtue of the "perfect conductor" argument: in this limit the lossless metal permittivity is mostly determined by the ω_P^2/ω^2 term, so the screening constant ε_∞ barely plays any role. In addition, Fig. S7 (within the SM [51]) presents the absolute (non-normalized) value of the coupling constant as a function of the meta-atom resonant frequency.

C. Polaritonic spectra with spheroidal meta-atoms

Next we analyze the behavior of the collective coupling constant in arrays of closely packed spheroidal meta-atoms, Fig. 6. This geometry is a good analytical approximation for elongated nanorods or nanodisks, which have been employed in a number of studies analyzing strong and ultrastrong coupling in systems of meta-atoms [32,39]. Elongating one of the axes of the spherical meta-atom affects its resonant properties and thus the collective coupling constant. The filling factor [Eq. (24)] of the lattice remains the same due to proportional scaling of the dimensions of the array. Violated spherical symmetry of a spheroidal meta-atom, however, couples orthogonal vector spherical harmonics of the electromagnetic field, which is why the quasinormal modes of a spheroidal meta-atom cannot be determined from a single characteristic equation, as in Eq. (5). Instead, an infinite chain of coupled equations must be used [61], which presents an excruciating problem.

For this reason, we obtain the eigenfrequency spectra of spheroidal meta-atoms numerically with the use of finite-element software COMSOL Multiphysics along with the specialized MAN package (Modal Analysis of Nanoresonators) [62]. The usage of additional software is desired because the built-in COMSOL eigenfrequency solver demonstrates insufficient convergence in problems with highly dispersive materials. We employ the QNMEig solver, which implements auxiliary-field technique for finding quasinormal modes (QNMs) [63]. The solver yields a set of modes, from which we select a valid QNM with lowest real part of eigenfrequency separating it from redundant so-called PML-modes. To that end we implement techniques described in Refs. [63,64] based on the locations of eigenfrequencies of different types in the complex plane.

Unlike the case of spherical meta-atoms with three frequency degenerate dipole transitions producing isotropic (direction-independent) energy spectra, the three orthogonal dipolar transitions of a spheroidal meta-atom are not, generally, degenerate, and would couple to the photon with different coupling strengths depending on its wave vector (propagation direction). Consequently, the resulting spectrum of polaritonic modes will be dependent on the propagation direction. However, in the case of large aspect ratios $AR \gg 1$, only one of the three dipolar transitions will interact substantially with the photon, as the other dipole resonances polarized along the shorter axes of the spheroid will be highly detuned from the relevant photonic energies. To keep the analysis simple, in the following we focus on coupling of the longer semi-axis dipole transition with the photonic field, and ignore the short-axis resonances of prolate meta-atoms.

Figures S8 and S9 (within the SM [51]) show the resulting transition dipole moments and normalized collective coupling strengths of prolate spheroids as a function of longer semi-axis a for a fixed plasma frequency $\omega_P = 10$ eV and varying aspect ratio (AR) (the special case of spherical meta-atoms is included as $AR = 1$). Overall, they demonstrate

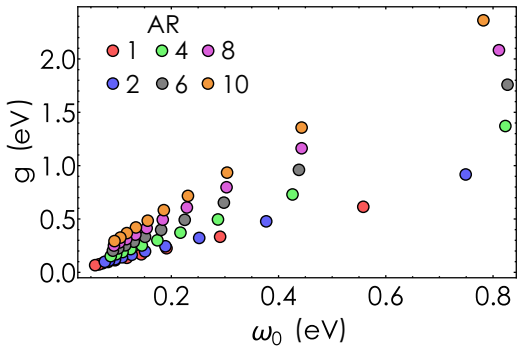

FIG. 7. Absolute values of the collective coupling strength in closely packed arrays of metallic spheroids as a function of the resonant meta-atom frequency ω_0. The data is obtained for a fixed $\omega_P = 10$ eV.

the behavior qualitatively similar to the ones obtained for spherical meta-atoms. Similarly to spheres, the normalized coupling constants quickly approaches an upper limit $\bar{\eta}$ with increasing longer semi-axis. This upper limit, however, is clearly different for every aspect ratio. Given the behavior of this constant for spherical meta-atoms, we expect it to be universal for any value of plasma frequency and only depend on the geometric AR of meta-atoms.

To that end, we study how the upper limit of the normalized coupling strength $\bar{\eta}$ depends on the spheroid aspect ratio. We approximately determine this limit as the maximal value of η for each AR from our data points, which is a good measure given how quickly the normalized coupling strength approaches the plateau. The resulting behavior of $\bar{\eta}$ shown in Fig. 6 reveals a nearly linear dependence of the upper limit of normalized coupling with the meta-atom aspect ratio, in particular reproducing the ultimate value of $\bar{\eta} \approx 1.2$ obtained for spherical meta-atoms. This suggests that prolate plasmonic meta-atoms are more efficient for achieving deep strong coupling between light and matter.

The above analysis clearly suggests that prolate spheroids are beneficial for reaching higher values of normalized coupling strength η. However, elongating a metallic nanoparticle comes at a price of red-shifting its resonances. Therefore, a natural question arises: What is the optimal shape (aspect ratio) of the metallic meta-atom that maximizes the absolute coupling constant $g_{\mathbf{k}}$ for a given resonant frequency ω_{pl}?

To that end, we utilize the same data and present the absolute value of the collective coupling constant in eV for all studied meta-atom aspect ratios (including the spherical case with AR $= 1$) as a function of the meta-atom resonant frequency, Fig. 7. The data allows to conclude that not only prolate spheroids offer high normalized coupling constant, but also yield the highest absolute value of the collective coupling constant for any given resonant energy. This observation suggests that highly elongated metallic meta-atoms are, perhaps, the optimal geometry for the purpose of realizing collective polaritonic states with the largest coupling constant and the mode splitting [34]. This behavior of elongated meta-atoms may be explained by a simple geometric argument. Transition dipole moment of the meta-atom μ_{01} is formed by the collective oscillations of the electron density inside the nanoparticle. better alignment of electron trajectories with the electric field of the photon therefore favors the collective coupling constant.

The data presented in Figs. 6 and S8 (within the SM [51]) may seem counterintuitive. Note that the data in Fig. S8 is plotted as a function of the longer semi-axis a for a series of aspect ratios. Correspondingly, in a meta-atom with a larger aspect ratio, although the electrons trajectories are better aligned with the electric field of the photon, the meta-atom *contains fewer electrons*. In turn, the transition dipole moment of an individual meta-atom actually decreases as a function of AR for fixed a. However, when these meta-atoms are combined in a lattice with a given volume filling factor f, elongated meta-atoms perform better in terms of the collective coupling strength.

Before concluding, we would like to emphasize the value of our results despite the number of crude simplifications and assumptions we have made in the model. Indeed, we assumed only electric dipole field-matter coupling, and included only the dipole-dipole interparticle interactions in the total Hamiltonian (mediated by the self-polarization P^2 term). At the same time, all the values of the collective coupling strength have been obtained in the limit of densely packed particles, where the multipolar interactions may become crucial. However, the developed formalism easily allows one to recalculate the coupling strength for less dense arrays with $f \ll 1$, where the interparticle interactions may be ignored. In this case, all the quantities will be equally scaled by a factor of $\sqrt{f}$ [see Eqs. (14) and (26)]. Therefore, the conclusion about the prolate meta-atoms yielding the highest coupling strength will remain true for any given filling factor of the meta-atom array, which is one the central findings of our paper.

V. CONCLUSIONS

To conclude, we have studied collective polaritonic states formed by arranged plasmonic meta-atoms interacting with the free space optical field. Almost linear scaling of the transition dipole moment of spherical meta-atom with its radius causes the collective coupling constant to quickly enter the ultrastrong and deep strong coupling regime before approaching a universal upper bound. The resulting bound is universal for all plasma frequencies and is determined only by the geometry of the meta-atom. The corresponding polaritonic energy spectra, calculated with the use of the developed Hamiltonian model, exhibit large values of mode splitting and polariton gaps. Similar analysis of the arrays of spheroid meta-atoms showed that the normalized collective coupling constant and it upper bound increases with the aspect ratio of elongated metallic meta-atoms. Furthermore, for any given resonant energy highly elongated spheroidal meta-atoms exhibit the highest absolute coupling constant. These results should open up prospects for realizing polariton states with artificial meta-atoms.

ACKNOWLEDGMENTS

Authors acknowledge fruitful discussion with Timur Shegai and Andrey Bogdanov. B.R. acknowledges fruitful discussions with Prof. Hans-Rudolf Jauslin and Prof. Gérard Colas des Francs. The Laboratoire Interdisciplinaire Carnot de

Bourgogne is a member of EIPHI Graduate School (Contract No. ANR- 17-EURE-0002). D.G.B. acknowledges support from the Ministry of Science and Higher Education of the Russian Federation (Agreement No. 075-15-2021-606), Russian Science Foundation (Grant No. 21-12-00316), and BASIS Foundation (Grant No. 22-1-3-2-1).

APPENDIX A: HAMILTONIAN DESCRIPTION OF A SINGLE META-ATOM

Let us first consider the case of an isolated spheroid nanoparticle as a single meta-atom, whose center-of-mass is placed at the origin. We start with the medium-assisted Maxwell equations,

$$\nabla\cdot\mathbf{D}=0,\quad \nabla\cdot\mathbf{B}=0,$$
$$\nabla\times\mathbf{E}=-\frac{\partial}{\partial t}\mathbf{B},\quad \nabla\times\mathbf{H}=\frac{\partial}{\partial t}\mathbf{D}. \tag{A1}$$

with the constitutive relations $\mathbf{D}=\epsilon_0\mathbf{E}+\mathbf{P}$ and $\mathbf{B}=\mu_0\mathbf{H}$. The medium is assumed to be finite and enclosed in a volume V_m, constituting a single meta-atom. Moreover, we assume the macroscopic polarization $\mathbf{P}$ having the form

$$\mathbf{P}(\mathbf{r},t)=\alpha(\mathbf{r})\mathbf{X}(\mathbf{r},t), \tag{A2}$$

where $\alpha(\mathbf{r})$ is a charge density corresponding to displaced charges and $\mathbf{X}$ is the associated vector field displacement. The polarization $\mathbf{P}(\mathbf{r},t)$ is localized within the volume V_m of the meta-atom, hence $\alpha(\mathbf{r})$ can be set to zero for $\mathbf{r}\notin V_m$. We also define the conjugate momentum $\mathbf{\Pi}_X$ of the displacement as

$$\mathbf{\Pi}_X(\mathbf{r},t)=\rho\frac{\partial}{\partial t}\mathbf{X}(\mathbf{r},t), \tag{A3}$$

where ρ is the volumic mass of the displaced electrons. The meta-atom is assumed to carry a single resonance at frequency ω_0 with neglected nonradiative damping, and the equation of motion for the meta-atom variables $\mathbf{X}$, $\mathbf{\Pi}_X$ is

$$\frac{\partial}{\partial t}\mathbf{\Pi}_X(\mathbf{r},t)+\omega_0^2\mathbf{X}(\mathbf{r},t)=\frac{\alpha(\mathbf{r})}{\rho}\mathbf{E}(\mathbf{r},t), \tag{A4}$$

so the polarization obeys, introducing $\beta(\mathbf{r})=\alpha^2(\mathbf{r})/\rho$,

$$\left(\frac{\partial^2}{\partial t^2}+\omega_0^2\right)\mathbf{P}(\mathbf{r},t)=\beta(\mathbf{r})\mathbf{E}(\mathbf{r},t). \tag{A5}$$

Since $\nabla\cdot\mathbf{B}=0$, Poincaré's lemma implies that $\mathbf{B}=\nabla\times\mathbf{A}$, where $\mathbf{A}$ is the vector potential. The same lemma applied to the Maxwell-Faraday equation implies that $\mathbf{E}+(\partial/\partial t)\mathbf{A}=-\nabla\Phi$, with the scalar potential Φ. Taking the divergence of this equality and using $\nabla\cdot\mathbf{D}=0$, we obtain

$$\frac{\partial}{\partial t}(\nabla\cdot\mathbf{A})=\nabla\cdot\left(\frac{\mathbf{P}_\parallel}{\epsilon_0}-\nabla\Phi\right), \tag{A6}$$

where $\mathbf{P}_\parallel$ is the irrotational (or longitudinal) part of the Helmholtz decomposition $\mathbf{P}=\mathbf{P}_\parallel+\mathbf{P}_\perp$. In virtue of Poincaré's lemma, the scalar potential can be chosen arbitrarily without changing Maxwell's equations. Hence we choose a potential Φ such that

$$\nabla\Phi=\frac{\mathbf{P}_\parallel}{\epsilon_0}, \tag{A7}$$

so $\nabla\cdot\mathbf{A}$ is time independent. To complete the construction of the Coulomb gauge, a gauge transformation $\mathbf{A}'=\mathbf{A}+\nabla F(\mathbf{r},t)$ can be found such that $\nabla\cdot\mathbf{A}(\mathbf{r},t_0)=0$ at some initial time t_0, ensuring that $\nabla\cdot\mathbf{A}=0$ at all times. For the Maxwell's equations (A1), the Coulomb gauge is therefore set by the two relations,

$$\nabla\cdot\mathbf{A}=0,$$
$$\nabla\Phi=\frac{\mathbf{P}_\parallel}{\epsilon_0}. \tag{A8}$$

We define the conjugate momentum $\mathbf{\Pi}_A=-\mathbf{D}$ of the vector potential $\mathbf{A}$, and we are going to show that the Hamiltonian

$$\begin{aligned}H=&\underbrace{\int_{V_m}d^3r\left(\frac{\mathbf{\Pi}_X^2}{2\rho}+\frac{1}{2}\rho\omega_0^2\mathbf{X}^2\right)}_{\text{meta-atom}}\\&+\underbrace{\int_{\mathbb{R}^3}d^3r\left(\frac{\mathbf{\Pi}_A^2}{2\epsilon_0}+\frac{(\nabla\times\mathbf{A})^2}{2\mu_0}\right)}_{\text{radiation}}\\&+\underbrace{\int_{V_m}d^3r\frac{\mathbf{P}^2}{2\epsilon_0}}_{\mathbf{P}^2\text{-term}}+\underbrace{\int_{V_m}d^3r\frac{\mathbf{P}\cdot\mathbf{\Pi}_A}{\epsilon_0}}_{\text{interaction}},\end{aligned} \tag{A9}$$

using the Hamilton equations, generates the dynamical equations (A1) and (A4). The Hamilton equations are

$$\frac{\partial}{\partial t}\mathbf{A}=\frac{\partial H}{\partial\mathbf{\Pi}_A}=\frac{\mathbf{\Pi}_A+\mathbf{P}}{\epsilon_0}=-\mathbf{E}_\perp, \tag{A10a}$$
$$\frac{\partial}{\partial t}\mathbf{\Pi}_A=-\frac{\partial H}{\partial\mathbf{A}}=\frac{\nabla^2\mathbf{A}}{\mu_0}, \tag{A10b}$$
$$\frac{\partial}{\partial t}\mathbf{X}=\frac{\partial H}{\partial\mathbf{\Pi}_X}=\frac{\mathbf{\Pi}_X}{\rho}, \tag{A10c}$$
$$\frac{\partial}{\partial t}\mathbf{\Pi}_X=-\frac{\partial H}{\partial\mathbf{X}}=-\rho\omega_0^2\mathbf{X}+\alpha\mathbf{E}. \tag{A10d}$$

Taking the curl of Eq. (A10a), we easily find the Maxwell-Faraday equation $\nabla\times\mathbf{E}_\perp\equiv\nabla\times\mathbf{E}=-(\partial/\partial t)\mathbf{B}$, while Eq. (A10b) retrieves the Maxwell-Ampère equation $\nabla\times\mathbf{H}=(\partial/\partial t)\mathbf{D}$, using $\mathbf{\Pi}_A=-\mathbf{D}$ and $\nabla^2\mathbf{A}=-\nabla\times\nabla\times\mathbf{A}$, since $\nabla\cdot\mathbf{A}=0$. The two remaining equations give identically the definition of the canonical momentum $\mathbf{\Pi}_X$ and Eq. (A4).

In fact, Hamiltonian (A9) corresponds to the famous Power-Zienau-Woolley Hamiltonian [65–67]. The kinetic term in $\mathbf{\Pi}_X^2$ corresponds to the motion of charges, while the potential term in $\mathbf{X}^2$ accounts for the restoring forces of infinitesimal dipoles. This term can in fact be injected in the $\mathbf{P}^2$ term when viewing the system solely as a localized system of charges. The Hamiltonian (A9) describes rigorously the interaction between a single meta-atom and electromagnetic radiation.

Next, we consider the case of a meta-atom whose size is negligible compared to the resonant wavelength λ_0, i.e., the quasistatic limit. Equation (A9) then reduces to

$$H \approx H_{\rm qs} = \int_{V_m} d^3r \left(\frac{\mathbf{\Pi}_X^2}{2\rho} + \frac{1}{2}\rho\omega_0^2 \mathbf{X}^2 \right) + \int_{V_m} d^3r \frac{\mathbf{P}_\parallel^2}{2\epsilon_0}. \tag{A11}$$

The $\mathbf{P}_\parallel^2$ term, involving the longitudinal part $\mathbf{P}_\parallel$ of the polarization, depends only on the charge displacement, hence on the dynamical variable $\mathbf{X}$. Therefore, the quasistatic Hamiltonian can be formally diagonalized and has the form

$$H_{\rm qs} = \int_{V_m} d^3r \left(\frac{\widetilde{\mathbf{\Pi}}_X^2}{2\rho} + \frac{1}{2}\rho\omega_{pl}^2 \widetilde{\mathbf{X}}^2 \right) \equiv \hbar\omega_{pl} b^\dagger b, \tag{A12}$$

where $b, b^\dagger$ are annihilation and creation operators for the corresponding dipolar plasmonic excitation of frequency ω_{pl}. We underline that this description does not involve any nonradiative processes such as Ohmic losses.

APPENDIX B: SINGLE META-ATOM COUPLED TO THE FREE-SPACE RADIATION FIELD

Using Hamiltonian (A12) and reintroducing the light-matter coupling, the total Hamiltonian (A9) takes the form

$$H \approx \hbar\omega_{pl} b^\dagger b + \sum_{\mathbf{k},\lambda} \hbar\omega_k a_{\mathbf{k}\lambda}^\dagger a_{\mathbf{k}\lambda} - \widehat{\boldsymbol{\mu}} \cdot \mathbf{E}(\mathbf{r}_0), \tag{B1}$$

where $a_{\mathbf{k}\lambda}, a_{\mathbf{k}\lambda}^\dagger$ are annihilation/creation operators for the radiation field, with wave vector $\mathbf{k}$ and transverse polarization index $\lambda = 1, 2$, and the polarization field operator of the meta-atom is approximated as a point dipole, $\mathbf{P} \approx \widehat{\boldsymbol{\mu}}\delta(\mathbf{r} - \mathbf{r}_0)$. The light-matter interaction term in $\mathbf{P} \cdot \Pi_A$ then turns into $-\widehat{\boldsymbol{\mu}} \cdot \mathbf{E}(\mathbf{r}_0)$, where the electric field $\mathbf{E}(\mathbf{r})$ is expressed in terms of the annihilation and creation operators

$$\mathbf{E}(\mathbf{r}) = i \sum_{\mathbf{k},\lambda} \sqrt{\frac{\hbar\omega_k}{2\epsilon_0 V}} \boldsymbol{\epsilon}_{\mathbf{k}\lambda} e^{-i\mathbf{k}\cdot\mathbf{r}} (a_{\mathbf{k}\lambda} - a_{-\mathbf{k}\lambda}^\dagger). \tag{B2}$$

In (B1), we also have neglected the Lamb shift induced by the term proportional to $\mathbf{P}_\perp^2$. We write Fermi's golden rule formula in the form

$$\gamma_{pl} = \frac{2\pi}{\hbar^2} \sum_{\mathbf{k},\lambda} |\langle 0, 1_{\mathbf{k}\lambda}| \widehat{\boldsymbol{\mu}} \cdot \mathbf{E}(\mathbf{r}_0) |1, \{0\}\rangle|^2 \delta(\omega_{pl} - \omega_k), \tag{B3}$$

where we introduced the eigenstates $|n, m_{\mathbf{k}\lambda}\rangle \equiv |n\rangle \otimes |m_{\mathbf{k}\lambda}\rangle$, $n, m = 0, 1$, where $|1_{\mathbf{k}\lambda}\rangle = a_{\mathbf{k}\lambda}^\dagger |\{0\}\rangle$ for the radiation field and $|1\rangle = b^\dagger|0\rangle$ for the meta-atom. Since we focus on *collective* ultrastrong light-matter coupling of a meta-atom supercrystal, we assume the effect of the ultrastrong light-matter coupling of a single meta-atom to be negligible and allow ourselves to use (B3). Next, injecting $\widehat{\boldsymbol{\mu}} = \boldsymbol{\mu}_{01}(b + b^\dagger)$ and Eq. (B2) in (B3), we obtain the formula (6) in the main text.

APPENDIX C: COLLECTIVE COUPLING

We proceed in deriving the Hamiltonian for a lattice of meta-atoms, regularly spaced and whose dipole moment is oriented along the same axis. In fact, the Hamiltonian has exactly the same form as (A9), if we assume that $\mathbf{X}$, $\mathbf{\Pi}_X$, and $\mathbf{P}$ describe all the meta-atoms at once. But since this vector field distribution is localized within each volume V_j of the jth meta-atom, we can express the Hamiltonian as

$$\begin{aligned} H = &\sum_j \int_{V_j} d^3r \left(\frac{\mathbf{\Pi}_j^2}{2\rho} + \frac{1}{2}\rho\omega_j^2 \mathbf{X}_j^2 \right) \\ &+ \int_{\mathbb{R}^3} d^3r \left(\frac{\mathbf{\Pi}_A^2}{2\epsilon_0} + \frac{(\nabla \times \mathbf{A})^2}{2\mu_0} \right) \\ &+ \sum_j \int_{V_j} d^3r \frac{\mathbf{P}_j^2}{2\epsilon_0} + \sum_j \int_{V_j} d^3r \frac{\mathbf{P}_j \cdot \mathbf{\Pi}_A}{\epsilon_0}, \end{aligned} \tag{C1}$$

where, this time, the variables $\mathbf{X}_j, \mathbf{\Pi}_j, \mathbf{P}_j$ are vector fields being localized only in meta-atom j. Since in this paper, we consider an infinite lattice with closely-packed meta-atoms (i.e., with the lattice constant being smaller than the resonant wavelength), it is convenient to perform the continuous limit by defining the collective polarization operator,

$$\mathbf{P} = \sum_{\mathbf{Q}} \frac{\boldsymbol{\mu}_N}{V_{\rm cell}} e^{-i\mathbf{Q}\cdot\mathbf{r}} (b_{\mathbf{Q}} + b_{-\mathbf{Q}}^\dagger), \tag{C2}$$

where $\boldsymbol{\mu}_N$ is the dipole moment enclosed in the lattice volume $V_{\rm cell}$. The polarization is expanded in a plane-wave basis, the operators $b_{\mathbf{Q}}, b_{\mathbf{Q}}^\dagger$ annihilate/create matter excitations with wave vector $\mathbf{Q}$ and they satisfy $[b_{\mathbf{Q}}, b_{\mathbf{Q}'}^\dagger] = \delta_{\mathbf{Q}\mathbf{Q}'}$. In this limit, and assuming that all meta-atoms are identical with $\omega_j = \omega_{pl}$, the Hamiltonian (C1) may be approximated as

$$\begin{aligned} H \approx &\sum_{\mathbf{Q}} \int_{\mathbb{R}^3} d^3r \left(\frac{\mathbf{\Pi}_{\mathbf{Q}}^2}{2\rho} + \frac{1}{2}\rho\omega_{pl}^2 \mathbf{X}_{\mathbf{Q}}^2 \right) \\ &+ \int_{\mathbb{R}^3} d^3r \left(\frac{\mathbf{\Pi}_A^2}{2\epsilon_0} + \frac{(\nabla \times \mathbf{A})^2}{2\mu_0} \right) \\ &+ \int_{\mathbb{R}^3} d^3r \frac{\mathbf{P}^2}{2\epsilon_0} + \int_{\mathbb{R}^3} d^3r \frac{\mathbf{P} \cdot \mathbf{\Pi}_A}{\epsilon_0}, \end{aligned} \tag{C3}$$

where this time all integrals run over all three-dimensional space $\mathbb{R}^3$. We also emphasize that the $\mathbf{P}^2$ term here represent the contact interaction between "point-like" meta-atoms, in contrast with the $\mathbf{P}^2$ term in, e.g., (A11), representing the dipole-dipole interaction between infinitesimal dipoles formed by the charge distribution within a single meta-atom.

Proceeding to the principle of correspondence to quantize the field, we identify

$$\int_{\mathbb{R}^3} d^3r \left(\frac{\mathbf{\Pi}_A^2}{2\epsilon_0} + \frac{(\nabla \times \mathbf{A})^2}{2\mu_0} \right) = \sum_{\mathbf{k},\lambda} \hbar\omega_k a_{\mathbf{k}\lambda}^\dagger a_{\mathbf{k}\lambda}, \tag{C4a}$$

$$\mathbf{D} = -\mathbf{\Pi}_A = i \sum_{\mathbf{k},\lambda} \sqrt{\frac{\epsilon_0 \hbar\omega_k}{2V}} \boldsymbol{\epsilon}_{\mathbf{k}\lambda} e^{-i\mathbf{k}\cdot\mathbf{r}} (a_{\mathbf{k}\lambda} - a_{-\mathbf{k}\lambda}^\dagger), \tag{C4b}$$

where $a_{\mathbf{k}\lambda}, a_{\mathbf{k}\lambda}^\dagger$ are annihilation/creation operators for the radiation field, with wave vector $\mathbf{k}$ and transverse polarization index $\lambda = 1, 2$. Writing the light-matter coupling term of

(C3), we find

$$\int_{\mathbb{R}^3} d^3r \frac{\mathbf{P}\cdot\mathbf{\Pi}_A}{\epsilon_0} = -i\sum_{\mathbf{k},\lambda}\sqrt{\frac{\hbar\omega_k}{2\epsilon_0 V}}(\boldsymbol{\mu}_N\cdot\boldsymbol{\epsilon}_{\mathbf{k}\lambda}) \times (a_{\mathbf{k}\lambda} - a^\dagger_{-\mathbf{k}\lambda})(b_{-\mathbf{k}} + b^\dagger_{\mathbf{k}}), \tag{C5}$$

where we have used $\int d^3r \exp(-i(\mathbf{Q}+\mathbf{k})) = V\delta_{\mathbf{Q},-\mathbf{k}}$. We see that the light-matter coupling implies that $\mathbf{k}$ vectors of the radiation field and of the matter excitations must coincide. We rewrite the Hamiltonian (C3) as

$$\begin{aligned} H = &\sum_{\mathbf{k}}\hbar\omega_{pl}b^\dagger_{\mathbf{k}}b_{\mathbf{k}} + \sum_{\mathbf{k},\lambda}\hbar\omega_k a^\dagger_{\mathbf{k}\lambda}a_{\mathbf{k}\lambda} \\ &+ \frac{\boldsymbol{\mu}_N^2}{2\epsilon_0 V}\sum_{\mathbf{k}}(b_{\mathbf{k}} + b^\dagger_{-\mathbf{k}})(b_{-\mathbf{k}} + b^\dagger_{\mathbf{k}}) \\ &- i\sum_{\mathbf{k},\lambda}\hbar g_{\mathbf{k}\lambda}(a_{\mathbf{k}\lambda} - a^\dagger_{-\mathbf{k}\lambda})(b_{-\mathbf{k}} + b^\dagger_{\mathbf{k}}). \end{aligned} \tag{C6}$$

APPENDIX D: HOPFIELD-BOGOLYUBOV DIAGONALIZATION

The Hamiltonian (C6), describing the interaction between the lattice of meta-atoms and electromagnetic radiation, can be written in the form $H = H_{\text{mat}} + H_{\text{light}} + H_{\text{light-mat}}$, where the matter part is

$$H_{\text{mat}} = \sum_{\mathbf{k}}\left(\hbar\omega_{pl}b^\dagger_{\mathbf{k}}b_{\mathbf{k}} + \frac{\boldsymbol{\mu}_N^2}{2\epsilon_0 V}(b_{\mathbf{k}} + b^\dagger_{-\mathbf{k}})(b_{-\mathbf{k}} + b^\dagger_{\mathbf{k}})\right). \tag{D1}$$

We next diagonalize H_{mat} with a Hopfield-Bogolyubov procedure. It consists in introducing the new (bosonic) operators $B_{\mathbf{k}} = xb_{\mathbf{k}} + yb^\dagger_{\mathbf{k}}$, with the normalization constraint $x^2 - y^2 = 1$ (assuming $x, y \in \mathbb{R}$), such that the eigenoperator problem $[B_{\mathbf{k}}, H_{\text{mat}}] = \Omega_{pl}B_{\mathbf{k}}$ is satisfied. This yields the 2×2 eigenvalue problem,

$$\begin{pmatrix} \omega_{pl} + U - \Omega_{pl} & -U \\ U & -\omega_{pl} - U - \Omega_{pl} \end{pmatrix}\begin{pmatrix} x \\ y \end{pmatrix} = 0, \tag{D2}$$

where $U = \frac{\boldsymbol{\mu}_N^2}{\hbar\epsilon_0 V}$. This is trivially solved by keeping the positive eigenfrequency solution,

$$\Omega_{pl} = \sqrt{\omega_{pl}^2 + \frac{2\boldsymbol{\mu}_N^2\omega_{pl}}{\hbar\epsilon_0 V}}. \tag{D3}$$

The diagonalized Hamiltonian is then

$$H_{\text{mat}} = \sum_{\mathbf{k}}\hbar\Omega_{pl}B^\dagger_{\mathbf{k}}B_{\mathbf{k}}, \tag{D4a}$$

$$B_{\mathbf{k}} = \frac{1}{2\sqrt{\omega_{pl}\Omega_{pl}}}((\omega_{pl}+\Omega_{pl})b_{\mathbf{k}} + (\omega_{pl}-\Omega_{pl})b^\dagger_{\mathbf{k}}). \tag{D4b}$$

Having diagonalized the matter part, the Hamiltonian (C6) becomes

$$H = \sum_{\mathbf{k}}\hbar\Omega_{pl}B^\dagger_{\mathbf{k}}B_{\mathbf{k}} + \sum_{\mathbf{k}}\hbar\omega_k a^\dagger_{\mathbf{k}}a_{\mathbf{k}} \tag{D5}$$

$$- i\sum_{\mathbf{k}}\hbar g_{\mathbf{k}}\sqrt{\frac{\omega_{pl}}{\Omega_{pl}}}(a_{\mathbf{k}} - a^\dagger_{-\mathbf{k}})(B_{-\mathbf{k}} + B^\dagger_{\mathbf{k}}). \tag{D6}$$

Because all meta-atoms are assumed to be dipoles with the same orientation, $\boldsymbol{\mu}_N = \mu_N\mathbf{u}_z$, we have eliminated the index λ from the Hamiltonian, since only the transverse magnetic polarization is interacting with the lattice. We can now diagonalize the full light-matter Hamiltonian by defining the polaritonic operators $\Pi_{\pm\mathbf{k}} = x_\pm a_{\mathbf{k}} + y_\pm a^\dagger_{\mathbf{k}} + m_\pm B_{\mathbf{k}} + h_\pm B^\dagger_{\mathbf{k}}$, satisfying the eigenoperator equation $[\Pi_{\pm\mathbf{k}}, H] = \Omega_\pm\Pi_{\pm\mathbf{k}}$, with the normalization constraint on the Hopfield coefficients: $x_\pm^2 - y_\pm^2 + m_\pm^2 - h_\pm^2 = 1$. The eigenvalue problem is then

$$\begin{pmatrix} \omega_k - \Omega_\pm & 0 & -i\tilde{g}_{\mathbf{k}} & i\tilde{g}_{\mathbf{k}} \\ 0 & -\omega_k - \Omega_\pm & i\tilde{g}_{\mathbf{k}} & -i\tilde{g}_{\mathbf{k}} \\ i\tilde{g}_{\mathbf{k}} & i\tilde{g}_{\mathbf{k}} & \Omega_{pl} - \Omega_\pm & 0 \\ i\tilde{g}_{\mathbf{k}} & i\tilde{g}_{\mathbf{k}} & 0 & -\Omega_{pl} - \Omega_\pm \end{pmatrix}\begin{pmatrix} x_\pm \\ y_\pm \\ m_\pm \\ h_\pm \end{pmatrix} = 0, \tag{D7}$$

where we introduced the shorthand notation $\tilde{g}_{\mathbf{k}} = g_{\mathbf{k}}\sqrt{\omega_{pl}/\Omega_{pl}}$. This eigenvalue problem is solved analytically. The polaritonic eigenfrequencies $\Omega_\pm$ are shown to be governed by a biquadratic equation

$$\left(\Omega_\pm^2 - \omega_k^2\right)\left(\Omega_\pm^2 - \Omega_{pl}^2\right) - 4\tilde{g}_{\mathbf{k}}^2\omega_k\Omega_{pl} = 0, \tag{D8}$$

whose positive solutions are

$$\Omega_\pm(\mathbf{k}) = \frac{1}{\sqrt{2}}\sqrt{\omega_k^2 + \Omega_{pl}^2 \pm \sqrt{\left(\omega_k^2 - \Omega_{pl}^2\right)^2 + 16\tilde{g}_{\mathbf{k}}^2\omega_k\Omega_{pl}}}. \tag{D9}$$

[1] D. L. Mills and E. Burstein, Polaritons: The electromagnetic modes of media, Rep. Prog. Phys. **37**, 817 (1974).

[2] P. Törmä and W. L. Barnes, Strong coupling between surface plasmon polaritons and emitters: A review, Rep. Prog. Phys. **78**, 013901 (2014).

[3] G. Khitrova, H. Gibbs, M. Kira, S. W. Koch, and A. Scherer, Vacuum Rabi splitting in semiconductors, Nat. Phys. **2**, 81 (2006).

[4] D. G. Baranov, M. Wersäll, J. Cuadra, T. J. Antosiewicz, and T. Shegai, Novel nanostructures and materials for strong light–matter interactions, ACS Photon. **5**, 24 (2018).

[5] J. P. Long and B. S. Simpkins, Coherent coupling between a molecular vibration and Fabry-Perot optical cavity to give hybridized states in the strong coupling limit, ACS Photon. **2**, 130 (2015).
[6] B. S. Simpkins, K. P. Fears, W. J. Dressick, B. T. Spann, A. D. Dunkelberger, and J. C. Owrutsky, Spanning strong to weak normal mode coupling between vibrational and Fabry-Pérot cavity modes through tuning of vibrational absorption strength, ACS Photon. **2**, 1460 (2015).
[7] D. Sanvitto and S. Kéna-Cohen, The road towards polaritonic devices, Nat. Mater. **15**, 1061 (2016).
[8] J. Galego, F. J. Garcia-Vidal, and J. Feist, Cavity-Induced Modifications of Molecular Structure in the Strong-Coupling Regime, Phys. Rev. X **5**, 041022 (2015).
[9] T. W. Ebbesen, Hybrid light–matter states in a molecular and material science perspective, Acc. Chem. Res. **49**, 2403 (2016).
[10] F. J. Garcia-Vidal, C. Ciuti, and T. W. Ebbesen, Manipulating matter by strong coupling to vacuum fields, Science **373**, eabd0336 (2021).
[11] A. Thomas, J. George, A. Shalabney, M. Dryzhakov, S. J. Varma, J. Moran, T. Chervy, X. Zhong, E. Devaux, C. Genet *et al.*, Ground-state chemical reactivity under vibrational coupling to the vacuum electromagnetic field, Angew. Chem. Int. Ed. **55**, 11462 (2016).
[12] F. Herrera and F. C. Spano, Cavity-Controlled Chemistry in Molecular Ensembles, Phys. Rev. Lett. **116**, 238301 (2016).
[13] B. Munkhbat, M. Wersäll, D. G. Baranov, T. J. Antosiewicz, and T. Shegai, Suppression of photo-oxidation of organic chromophores by strong coupling to plasmonic nanoantennas, Sci. Adv. **4**, eaas9552 (2018).
[14] A. Thomas, L. Lethuillier-Karl, K. Nagarajan, R. M. Vergauwe, J. George, T. Chervy, A. Shalabney, E. Devaux, C. Genet, J. Moran, and T. W. Ebbesen, Tilting a ground-state reactivity landscape by vibrational strong coupling, Science **363**, 615 (2019).
[15] V. N. Peters, M. O. Faruk, J. Asane, R. Alexander, A. P. D'angelo, S. Prayakarao, S. Rout, and M. Noginov, Effect of strong coupling on photodegradation of the semiconducting polymer P3HT, Optica **6**, 318 (2019).
[16] K. Stranius, M. Hertzog, and K. Börjesson, Selective manipulation of electronically excited states through strong light–matter interactions, Nat. Commun. **9**, 2273 (2018).
[17] J. Galego, F. J. Garcia-Vidal, and J. Feist, Suppressing photochemical reactions with quantized light fields, Nat. Commun. **7**, 13841 (2016).
[18] L. A. Martínez-Martínez, R. F. Ribeiro, J. Campos-González-Angulo, and J. Yuen-Zhou, Can ultrastrong coupling change ground-state chemical reactions? ACS Photon. **5**, 167 (2018).
[19] J. Feist, J. Galego, and F. J. Garcia-Vidal, Polaritonic chemistry with organic molecules, ACS Photon. **5**, 205 (2018).
[20] J. Fregoni, F. J. Garcia-Vidal, and J. Feist, Theoretical challenges in polaritonic chemistry, ACS Photon. **9**, 1096 (2022).
[21] C. Schäfer, M. Ruggenthaler, H. Appel, and A. Rubio, Modification of excitation and charge transfer in cavity quantum-electrodynamical chemistry, Proc. Natl. Acad. Sci. USA **116**, 4883 (2019).
[22] C. Schäfer, J. Flick, E. Ronca, P. Narang, and A. Rubio, Shining light on the microscopic resonant mechanism responsible for cavity-mediated chemical reactivity, Nat. Commun. **13**, 7817 (2022).
[23] J. Yuen-Zhou, W. Xiong, and T. Shegai, Polariton chemistry: Molecules in cavities and plasmonic media, J. Chem. Phys. **156**, 030401 (2022).
[24] C. E. Platts, M. A. Kaliteevski, S. Brand, R. A. Abram, I. V. Iorsh, and A. V. Kavokin, Whispering-gallery exciton polaritons in submicron spheres, Phys. Rev. B **79**, 245322 (2009).
[25] A. Canales, D. G. Baranov, T. J. Antosiewicz, and T. Shegai, Abundance of cavity-free polaritonic states in resonant materials and nanostructures, J. Chem. Phys. **154**, 024701 (2021).
[26] P. A. Thomas, K. S. Menghrajani, and W. L. Barnes, Cavity-free ultrastrong light-matter coupling, J. Phys. Chem. Lett. **12**, 6914 (2021).
[27] R. Chikkaraddy, B. De Nijs, F. Benz, S. J. Barrow, O. A. Scherman, E. Rosta, A. Demetriadou, P. Fox, O. Hess, and J. J. Baumberg, Single-molecule strong coupling at room temperature in plasmonic nanocavities, Nature (London) **535**, 127 (2016).
[28] T. Neuman, R. Esteban, D. Casanova, F. J. García-Vidal, and J. Aizpurua, Coupling of molecular emitters and plasmonic cavities beyond the point-dipole approximation, Nano Lett. **18**, 2358 (2018).
[29] T. P. Rossi, T. Shegai, P. Erhart, and T. J. Antosiewicz, Strong plasmon-molecule coupling at the nanoscale revealed by first-principles modeling, Nat. Commun. **10**, 3336 (2019).
[30] M. Kuisma, B. Rousseaux, K. M. Czajkowski, T. P. Rossi, T. Shegai, P. Erhart, and T. J. Antosiewicz, Ultrastrong coupling of a single molecule to a plasmonic nanocavity: A first-principles study, ACS Photon. **9**, 1065 (2022).
[31] R. Ameling and H. Giessen, Cavity plasmonics: Large normal mode splitting of electric and magnetic particle plasmons induced by a photonic microcavity, Nano Lett. **10**, 4394 (2010).
[32] A. Bisht, J. Cuadra, M. Wersall, A. Canales, T. J. Antosiewicz, and T. Shegai, Collective strong light-matter coupling in hierarchical microcavity-plasmon-exciton systems, Nano Lett. **19**, 189 (2019).
[33] A. Konrad, A. M. Kern, M. Brecht, and A. J. Meixner, Strong and coherent coupling of a plasmonic nanoparticle to a subwavelength Fabry–Pérot resonator, Nano Lett. **15**, 4423 (2015).
[34] M. Hertzog, B. Munkhbat, D. Baranov, T. Shegai, and K. Boörjesson, Enhancing vibrational light–matter coupling strength beyond the molecular concentration limit using plasmonic arrays, Nano Lett. **21**, 1320 (2021).
[35] M. Schäferling, D. Dregely, M. Hentschel, and H. Giessen, Tailoring Enhanced Optical Chirality: Design Principles for Chiral Plasmonic Nanostructures, Phys. Rev. X **2**, 031010 (2012).
[36] D. G. Baranov, B. Munkhbat, N. O. Länk, R. Verre, M. Käll, and T. Shegai, Circular dichroism mode splitting and bounds to its enhancement with cavity-plasmon-polaritons, Nanophotonics **9**, 283 (2020).
[37] D. G. Baranov, C. Schäfer, and M. V. Gorkunov, Toward molecular chiral polaritons, ACS Photon. (2023), doi: 10.1021/acsphotonics.2c02011.
[38] C. Schäfer and D. G. Baranov, Chiral polaritonics: Analytical solutions, intuition, and use, J. Phys. Chem. Lett. **14**, 3777 (2023).
[39] D. G. Baranov, B. Munkhbat, E. Zhukova, A. Bisht, A. Canales, B. Rousseaux, G. Johansson, T. J. Antosiewicz, and T. Shegai, Ultrastrong coupling between nanoparticle plasmons and cavity photons at ambient conditions, Nat. Commun. **11**, 2715 (2020).

[40] S. Rajabali, S. Markmann, E. Jöchl, M. Beck, C. A. Lehner, W. Wegscheider, J. Faist, and G. Scalari, An ultrastrongly coupled single terahertz meta-atom, Nat. Commun. **13**, 2528 (2022).
[41] S. Gambino, M. Mazzeo, A. Genco, O. Di Stefano, S. Savasta, S. Patanè, D. Ballarini, F. Mangione, G. Lerario, D. Sanvitto, and G. Gigli, Exploring light-matter interaction phenomena under ultrastrong coupling regime, ACS Photon. **1**, 1042 (2014).
[42] N. S. Mueller, Y. Okamura, B. G. Vieira, S. Juergensen, H. Lange, E. B. Barros, F. Schulz, and S. Reich, Deep strong light–matter coupling in plasmonic nanoparticle crystals, Nature (London) **583**, 780 (2020).
[43] C. Ciuti, G. Bastard, and I. Carusotto, Quantum vacuum properties of the intersubband cavity polariton field, Phys. Rev. B **72**, 115303 (2005).
[44] S. De Liberato, Light-Matter Decoupling in the Deep Strong Coupling Regime: The Breakdown of the Purcell Effect, Phys. Rev. Lett. **112**, 016401 (2014).
[45] P. Forn-Díaz, L. Lamata, E. Rico, J. Kono, and E. Solano, Ultrastrong coupling regimes of light-matter interaction, Rev. Mod. Phys. **91**, 025005 (2019).
[46] S. Lamowski, C.-R. Mann, F. Hellbach, E. Mariani, G. Weick, and F. Pauly, Plasmon polaritons in cubic lattices of spherical metallic nanoparticles, Phys. Rev. B **97**, 125409 (2018).
[47] E. B. Barros, B. G. Vieira, N. S. Mueller, and S. Reich, Plasmon polaritons in nanoparticle supercrystals: Microscopic quantum theory beyond the dipole approximation, Phys. Rev. B **104**, 035403 (2021).
[48] C. F. Bohren and D. R. Huffman, *Absorption and Scattering of Light by Small Particles* (Wiley, Hoboken, NJ, 2004) p. 530.
[49] L. Novotny and B. Hecht, *Principles of Nano-Optics* (Cambridge University Press, Cambridge, 2012).
[50] Y. Todorov, Dipolar quantum electrodynamics theory of the three-dimensional electron gas, Phys. Rev. B **89**, 075115 (2014).
[51] See Supplemental Material at http://link.aps.org/supplemental/10.1103/PhysRevB.108.075417 for the additional calculated data on the polaritonic properties of spherical and nonspherical meta-atoms.
[52] E. S. Barnard, J. S. White, A. Chandran, and M. L. Brongersma, Spectral properties of plasmonic resonator antennas, Opt. Express **16**, 16529 (2008).
[53] L. Novotny, Effective Wavelength Scaling for Optical Antennas, Phys. Rev. Lett. **98**, 266802 (2007).
[54] T. A. Milligan, *Modern Antenna Design* (John Wiley & Sons, Hoboken, NJ, 2005).
[55] Y. Todorov and C. Sirtori, Intersubband polaritons in the electrical dipole gauge, Phys. Rev. B **85**, 045304 (2012).
[56] Y. Todorov, Dipolar quantum electrodynamics of the two-dimensional electron gas, Phys. Rev. B **91**, 125409 (2015).
[57] C. Schäfer, M. Ruggenthaler, V. Rokaj, and A. Rubio, Relevance of the quadratic diamagnetic and self-polarization terms in cavity quantum electrodynamics, ACS Photon. **7**, 975 (2020).
[58] J. Casanova, G. Romero, I. Lizuain, J. J. García-Ripoll, and E. Solano, Deep Strong Coupling Regime of the Jaynes-Cummings Model, Phys. Rev. Lett. **105**, 263603 (2010).
[59] N. K. Langford, R. Sagastizabal, M. Kounalakis, C. Dickel, A. Bruno, F. Luthi, D. J. Thoen, A. Endo, and L. DiCarlo, Experimentally simulating the dynamics of quantum light and matter at deep-strong coupling, Nat. Commun. **8**, 1715 (2017).
[60] J. Hopfield, Theory of the contribution of excitons to the complex dielectric constant of crystals, Phys. Rev. **112**, 1555 (1958).
[61] S. Asano and G. Yamamoto, Light scattering by a spheroidal particle, Appl. Opt. **14**, 29 (1975).
[62] T. Wu, D. Arrivault, W. Yan, and P. Lalanne, Modal analysis of photonic and plasmonic resonators: User guide for the MAN program, Comput. Phys. Commun. **284**, 108627 (2023).
[63] W. Yan, R. Faggiani, and P. Lalanne, Rigorous modal analysis of plasmonic nanoresonators, Phys. Rev. B **97**, 205422 (2018).
[64] P. Lalanne, W. Yan, K. Vynck, C. Sauvan, and J. P. Hugonin, Light interaction with photonic and plasmonic resonances, Laser Photonics Rev. **12**, 1700113 (2018).
[65] C. Cohen-Tannoudji, J. Dupont-Roc, and G. Grynberg, *Photons and Atoms: Introduction to Quantum Electrodynamics* (John Wiley, Hoboken, NJ, 1997).
[66] D. L. Andrews, G. A. Jones, A. Salam, and R. G. Woolley, Perspective: Quantum Hamiltonians for optical interactions, J. Chem. Phys. **148**, 040901 (2018).
[67] A. Vukics, G. Kónya, and P. Domokos, The gauge-invariant lagrangian, the Power–Zienau-Woolley picture, and the choices of field momenta in nonrelativistic quantum electrodynamics, Sci. Rep. **11**, 16337 (2021).